



Article

# Role of the South Asian High in the Onset Process of the Asian Summer Monsoon during Spring-to-Summer Transition

Wei Wei <sup>1,2,3,\*</sup> , Yuting Wu <sup>1,3</sup>, Song Yang <sup>1,3</sup> and Wen Zhou <sup>4</sup> 

<sup>1</sup> School of Atmospheric Sciences, and Guangdong Province Key Laboratory for Climate Change and Natural Disaster Studies, Sun Yat-sen University, Zhuhai 519082, China; wuyt9@mail2.sysu.edu.cn (Y.W.); yangsong3@mail.sysu.edu.cn (S.Y.)

<sup>2</sup> Key Laboratory of Meteorological Disaster of Ministry of Education, Nanjing University of Information Science and Technology, Nanjing 210044, China

<sup>3</sup> Southern Marine Science and Engineering Guangdong Laboratory (Zhuhai), Zhuhai 519000, China

<sup>4</sup> Guy Carpenter Asia-Pacific Climate Impact Centre, School of Energy and Environment, City University of Hong Kong, Hong Kong 00852, China; wenzhou@cityu.edu.hk

\* Correspondence: weiwei48@mail.sysu.edu.cn; Tel.: +86-20-8411-1566

Received: 16 April 2019; Accepted: 30 April 2019; Published: 1 May 2019



**Abstract:** The evolution of the South Asian high (SAH) and its role in the onset process of the Asian summer monsoon (ASM) during the spring-to-summer transition are investigated by using the NCEP-DOE reanalysis II dataset, with a focus on climatology and interannual time scales. Our results show four sudden changes of the SAH in its Northwestward evolution from the Western Pacific to the South China Sea (SCS), the Indochina Peninsula and the South Asian plateaus, coincide with the ASM onset over the Bay of Bengal, the SCS, and the Indian summer monsoon region. The physical process for the mutual promotion between the SAH and ASM rainfall is revealed. Accompanying the SAH evolution, the upper-level Easterly wind along the Southern flank and the upper-level divergence associated with the SAH shift Northwestward accordingly. The upper-level Easterly wind coordinates with the lower-level Southwesterly wind, and forms the summer circulation structure in the ASM regions gradually. Besides, the upper-level divergence associated with the SAH enhances ascending motion in ASM regions and increases the monsoon rainfall accordingly. Subsequently, the latent heat associated with the monsoon rainfall in the monsoon onset region excites an anticyclone to its Northwest in the upper level, which keeps strengthening the SAH and moving it Northwestward. This mutual promotion between the SAH and ASM rainfall can be affected by the sea surface temperatures (SSTs) in the Western Pacific and tropical Indian Ocean in the previous month. Colder (warmer) SSTs over the Western Pacific and inactive (active) convection over the Southern Philippines suppress (favor) the Northwestward development of the SAH in late April. In addition, the warmer (colder) SSTs in the tropical Indian Ocean excites anomalous anticyclone (cyclone) in the upper level near the equator, which keeps the SAH in the lower latitudes (promotes the SAH to the North), and delays (advances) the mutual promotion between the SAH and ASM rainfall. As a result, the entire ASM onset process is later (earlier) than normal.

**Keywords:** South Asian high; spring-to-summer transition; Asian summer monsoon; monsoon onset

## 1. Introduction

The South Asian high (SAH) is the most intense and stable upper-level circulation system during boreal summer [1,2]. It is one of the major components of the Asian summer monsoon (ASM) system [3,4]. Previous studies have revealed that the SAH plays an important role in the ASM

onset, active and break, and in the monsoon rainfall variability on different time scales during boreal summer [5–17]. The Easterly jet stream on the Southern flank of the SAH is a key factor affecting the Indian summer monsoon (ISM) onset and rainfall variability [1,18–24]. The upper-level Easterly wind and the lower-level Southwesterly wind jointly form the baroclinic summer-type vertical structure over the ISM region. Besides, the SAH interacts with the Western North Pacific subtropical high (WNPSH) and exerts its impact on the East Asian summer monsoon (EASM) [6,25–27]. When the SAH shifts Eastward and the WNPSH extends Westward [1,2,26–30], the meridional circulation is strengthened, which results in increased rainfall over the Yangtze River valley in China, and decreased rainfall over Southern and Northern China [6]. Moreover, the SAH has been identified as an important bridge connecting the ISM and the EASM on inter-annual time scales [6,7]. The physical process for the interaction among the SAH, the ISM rainfall and EASM rainfall has been revealed: When the ISM is stronger (weaker) than normal, the positive (negative) condensation latent heat anomaly associated with increasing (decreasing) monsoon rainfall over the ISM region excites an anomalous anticyclone to its West (east) and an anomalous cyclone to its East (west), leading to the Westward (eastward) shift of the SAH. The circulation anomalies associated with the zonal movement of the SAH further influence the summer rainfall anomalies in China [6]. On the contrary, the rainfall anomalies in the Yangtze River valley have feedback effect on the SAH, and result in a Southeast-Northwest movement of the SAH [7]. These studies indicate that the SAH is important for the ASM and can act as a bridge connecting the ASM subsystems during summer. However, the role of the SAH in connecting different ASM subsystems during the spring-to-summer transition is still unclear.

During the spring-to-summer transition, the ASM evolution process begins with the Bay of Bengal (BOB) monsoon onset, with a burst of monsoon rainfall in that region [31]. Then, the monsoon rainfall region expands Northeastward and Northwestward gradually, inducing the South China Sea (SCS) monsoon onset in mid-May and then the ISM onset in early-June. The monsoon onset over the SCS is considered as the beginning of the EASM [32–34]. Two weeks before the ASM onset, the SAH is generated over the SCS. It is mainly affected by a negative vorticity source produced by a burst of convection over the Southern Philippines [35,36]. After that, the zonal asymmetric potential vorticity forcing leads to a Westward development of the SAH [37]. The upper-level divergence on the Southwest of the SAH provides favorable pumping for the development of the lower-level vortex, leading to the monsoon onset over the BOB [36–40]. For the ISM onset, the Easterly wind in the upper level and the Southwesterly wind in the lower level jointly forms the baroclinic summer-type vertical structure over the ISM region [1,18–24]. The establishment of Easterly wind over the ISM region is closely related with the Northwestward advancement of the SAH. However, the relationship between the evolution of the SAH and the ISM onset progress is seldom mentioned. For the SCS monsoon onset, one of the indicators is the reversal of the 850-hPa zonal winds over the SCS from Easterly to Westerly [41–43]. The retreat of the WNPSH from the SCS is also regarded as an important signal of the SCS monsoon onset [41–43]. Moreover, the vertical shear of zonal wind can reflect the establishment and intensity of the tropical monsoon [44,45]. Actually, it can also reflect the configuration of the SAH in the upper levels and the WNPSH in the mid and lower levels. However, a large number of studies focus on the mid- and lower-level monsoon systems, and only limited effort has been devoted to investigating the effect of the upper-level SAH on the monsoon onset process. These studies show that the development of the SAH is closely related to the individual monsoon onsets over Asia. However, the question remains open as to the role the SAH plays in the entire tropical ASM evolution.

The external forcing such as sea surface temperature (SST) exerts significant influence on the variation of the SAH. On the inter-annual time scales, the intensity and location of the SAH can be affected by the SSTs in the tropical Indian Ocean and Pacific Ocean during boreal summer [46,47]. The long-term trend in the Southward extension of the SAH is closely related to the warming trend in the SST of the Indian Ocean [48,49]. The warm SST in the tropical Indian Ocean excites an anomalous upper-level anticyclone in the tropics, which results in a Southward extension of the SAH. Besides, the El Niño-Southern Oscillation (ENSO) imposes a great impact on the convection near the Philippines

and over the Indochina Peninsula during spring, facilitating the development of the SAH over the SCS and the Indochina Peninsula, leading the onsets of the ASM [39,40].

As mentioned above, previous studies pointed out the role of the SAH in the individual monsoon onsets over Asia, but seldom discussed the physical mechanism for the mutual promotion between the SAH and ASM rainfall in the entire tropical ASM evolution. In this study, we focus on the role of the SAH in promoting the ASM onsets during the spring-to-summer transition, and reveal the mechanism for the mutual promotion between the SAH and the ASM rainfall in the entire tropical ASM onset process. In Section 2, we describe the data and methods used in this study. The climatological SAH evolution during the spring-to-summer transition and its relation with the ASM onset progress are presented in Section 3. The key factor influencing the SAH evolution and the physical process behind the mutual promotion of the SAH and the ASM rainfall are also investigated in Section 3. Summary of this study is provided in Section 4.

## 2. Data and Methods

The data used in the study include: daily reanalysis of  $2.5^\circ \times 2.5^\circ$  horizontal resolution for 1979–2017 from the National Centers for Environmental Prediction-Department of Energy (NCEP-DOE) Reanalysis Version II data [50]; daily outgoing longwave radiation (OLR) data for 1979–2015 on  $2.5^\circ \times 2.5^\circ$  grid from the polar-orbiting series of satellites of the National Oceanic and Atmospheric Administration (NOAA) [51]; pentad Global Precipitation Climatology Project (GPCP) Version 2.2 data of  $2.5^\circ \times 2.5^\circ$  horizontal resolution from 1979 to 2017 provided by the NASA (<https://precip.gsfc.nasa.gov/>). We focus on the pentad (5-day) mean circulation during the spring-to-summer transition from March to June.

To quantify the Asian monsoon establishing process, we used the reversal of the meridional temperature gradient ( $MTG = \partial T / \partial y$ ) to identify the monsoon onset pentad in different regions of Asia [40,52–55]. According to the thermal wind relation:

$$\frac{\partial U}{\partial p} = \frac{R}{f p} \left( \frac{\partial T}{\partial y} \right) \quad (1)$$

the vertical wind shear depends on MTG. A positive MTG indicates the summer-type circulation structure. While a negative MTG implies the winter-type circulation structure. So, the transition of MTG from negative to positive in the mid-upper troposphere indicates the circulation changes from the winter type to the summer type, namely, the onset of the ASM circulation [52]. Here, we calculate the vertical integration of pentad-mean air temperature in the upper troposphere of 200–500 hPa and identify the monsoon onset pentad as the reversal pentad of MTG from negative to positive. Monsoon onsets over the typical tropic monsoon regions of the BOB ( $5^\circ$ – $15^\circ$  N,  $90^\circ$ – $100^\circ$  E), the SCS ( $10^\circ$ – $20^\circ$  N,  $110^\circ$ – $120^\circ$  E), and the ISM region ( $10^\circ$ – $20^\circ$  N,  $60^\circ$ – $85^\circ$  E) are considered as important steps in the ASM evolution.

The Northwestward shift of the SAH from the Western Pacific to the South Asian plateaus is a distinguishing feature in the SAH evolution during the spring-to-summer transition. We calculate the location of the pentad mean SAH to quantify its Northwestward propagation in the spring-to-summer transition. During early spring, when the anticyclone is over the Western tropical Pacific, weak intensity and small horizontal gradient in the SAH induce inaccuracy in locating the SAH by the maximum intensity center, which is only one grid point in the SAH ( $Z_{cent}$ ). So, we calculate the position of the SAH gravity center to depict the Northwestward advancement of the SAH and compare it with the maximum intensity center of the SAH. The gravity center is defined as the weighted average geopotential height in the region enclosed by the  $Z_{cent}$ -10 gpm contour at 200 hPa ( $Z_{200}$ ) in the regions

of 5°–60° N, 35°–130° E. The weight is defined as the ratio of the geopotential height in each grid cell to the domain average of geopotential height:

$$\begin{cases} x_0 = \frac{\sum_1^N z_{i,j} \cdot x_i}{\sum_1^N z_{i,j}} \\ y_0 = \frac{\sum_1^N z_{i,j} \cdot y_j}{\sum_1^N z_{i,j}} \end{cases}, z_{i,j} = \begin{cases} z_{i,j}, & z_{i,j} > z_{cent} - 10 \text{ gpm} \\ 0, & z_{i,j} < z_{cent} - 10 \text{ gpm} \end{cases} \quad (2)$$

where  $z_{i,j}$  denotes the relative vorticity at grid cell  $(x_i, y_j)$  and  $N$  is the number of grid cells enclosed by the  $Z_{cent}-10$  gpm contour.

### 3. Results

#### 3.1. Evolution of SAH and its Relation with ASM Onset Process

The annual cycle of the SAH moving track is shown in Figure 1. There are four stages of the SAH evolution in its annual cycle. During stage one (from January to March) and stage three (from July to August), the SAH is steady over the Western Pacific and the South Asian plateaus, respectively. During stage two (from April to June) and stage four (from September to December), the SAH is in the fast growing and decaying period with rapid Northwestward and Southeastward movement, respectively. The distinction between the stable stages and moving stages of the SAH is much more clearly shown by the moving track of the weighted average center (gravity center; Figure 1b) than by the maximum center (Figure 1a). The SAH gravity centers are more concentrated during the stable stages, compared with the maximum centers.

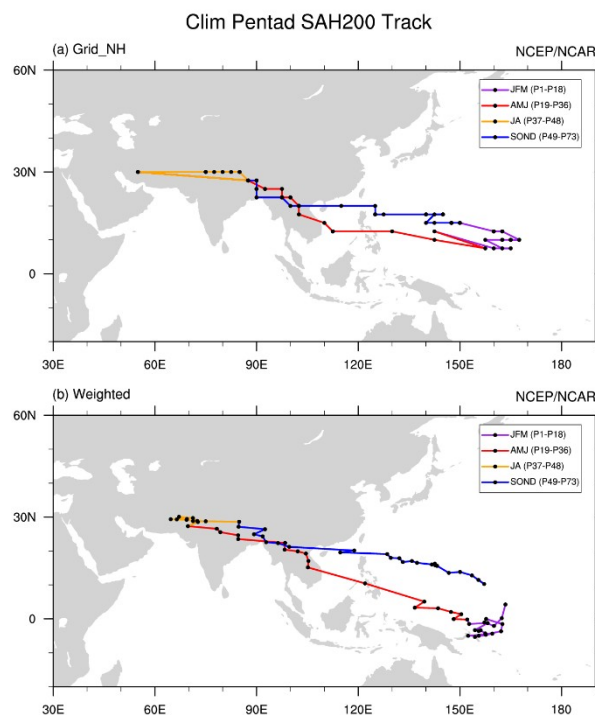


**Figure 1.** The climatological SAH track from Pentad 1 to Pentad 73. Black dots indicate (a) the maximum center of the SAH and (b) the gravity center of the SAH. Purple, red, orange, and blue lines indicate the track of the SAH during January–March, April–June, July–August, and September–December, respectively.

Focusing on the spring-to-summer transition (stage two), the SAH is moving fast from the Western Pacific to the South Asian plateaus (Figure 1). The evolution of the SAH in each pentad during April and May (P19–P30) is shown in Figure 2. In early April (P19–P20), the upper-level anticyclone is located

over the Western Pacific. The Western ridge of the SAH (12460-gpm contour) is near 125° E, to the East of the Philippines. On Pentad 21, the SAH is enhanced and shifts Westward rapidly with its Western ridge near 110° E, reaching the East coast of the Indochina Peninsula. The Southern SCS is controlled by the Western SAH. Then, the SAH keeps moving Westward. On Pentad 23, the SAH is further strengthened with its center near 12° N, 113° E over the SCS. On Pentad 27, the SAH stations over the central Indochina Peninsula, and then keeps its rapid strengthening and moving Northwestward from Pentad 27 to Pentad 30. On Pentad 30, the SAH shifts to the Northern Indochina Peninsula with its center strengthened to over 12,500 gpm.

The establishment of the summer circulation over the ASM regions corresponds to the evolution of the SAH. The summer circulation, indicated by positive MTG, appears to the South of the SAH ridge-line (Figure 2). In April from Pentad 19 to Pentad 23, the positive MTG region presents a belt-like pattern located over 0–5° N from the Indian Ocean to the Western Pacific. On Pentad 24, the belt-like pattern of the positive MTG turns in to a triangle pattern, implying the ASM onset first occurs over the Southeastern BOB. Then the triangle region expands Northward gradually from Pentad 24 to Pentad 30, indicating the steady Northward advance of the monsoonal circulation over tropical Asia. Meanwhile, the zero isoline of the MTG almost coincides with the ridge-line of the SAH, especially in its Western part. On Pentad 30, the zero MTG isoline almost coincide with the ridge line of the whole SAH. This indicates a close relationship between the Northward shift of the SAH and the Northward advancement of the ASM.

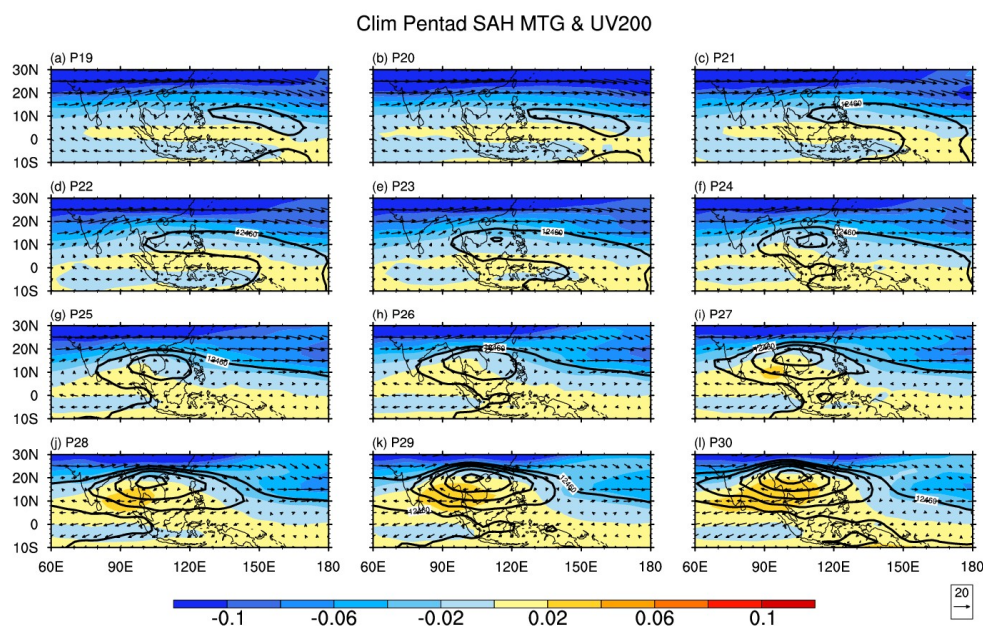


**Figure 2.** Climatological evolution of the SAH (contours of 12,460, 12,470, 12,480, 12,490, and 12,500 gpm), MTG (shading; K) and horizontal winds (vectors; m/s) at 200 hPa from Pentad 19 to Pentad 30 (a–l).

The close relationship between SAH evolution and the ASM onset can be found in the sudden changes of the SAH in its annual cycle. The annual cycles of the SAH intensity and location are shown in Figure 3a–c. Rapid enhancement and Northwestward shift of the SAH are obvious during the spring-to-summer transition (Pentad 19 to Pentad 36). Focus on the spring-to-summer transition (Figure 3d–i), there are four sudden changes on pentads 23, 27, 29 and 31, respectively. On Pentad 23, the SAH shifts Westward suddenly with its maximum center to the West of 120° E over the SCS (Figure 3i). On Pentad 27, the grid number in the region enclosed by the  $Z_{cent}-10$  gpm contour sudden decreases from 95 to 49 (Figure 3d). It means that the SAH intensity is strengthened rapidly with a sudden increase in the horizontal gradient of geopotential height at 200 hPa. The location of the SAH gravity center sudden shifts from the Southern Philippines (10.45° N, 122° E) to the Southern Indochina

Peninsula (15.15° N, 105.15° E) (Figures 2b and 3e,f). The sudden enhancement and Northwestward shift of the SAH center imply that the summer-type SAH is formed. On Pentad 29, the SAH maximum center shifts to 20° N with the intensity strengthened to over 12500 gpm (Figure 3g,h). On Pentad 31, both the maximum center and the gravity center shift to the Northwest of 20° N, 100° E. These four sudden changes imply the interaction between the SAH and ASM onset. After Pentad 37, the evolution of the SAH turns from moving stage to stable stage with robust and slightly varied intensity (Figure 3a,d,g) and the SAH center hovers around 27.5° N–30° N (Figures 1 and 3b,e,h) over the plateaus (Figure 1).

Figure 4 shows the ASM onset process during the spring-to-summer transition in terms of MTG transition from negative to positive. The triangle pattern of the MTG is obvious over the tropical ASM region. This pattern indicates the ASM onset firstly occurs over the BOB, and then advances Northeastward and Northwestward gradually. Focusing on the three tropical ASM regions, the monsoon onsets over the BOB, the SCS and the ISM are on pentads 25, 28, and 30, respectively. It is clear that the sudden changes of the SAH occur one or two pentads before or after the ASM onset in different regions, implying the mutual promotion between the SAH and ASM.

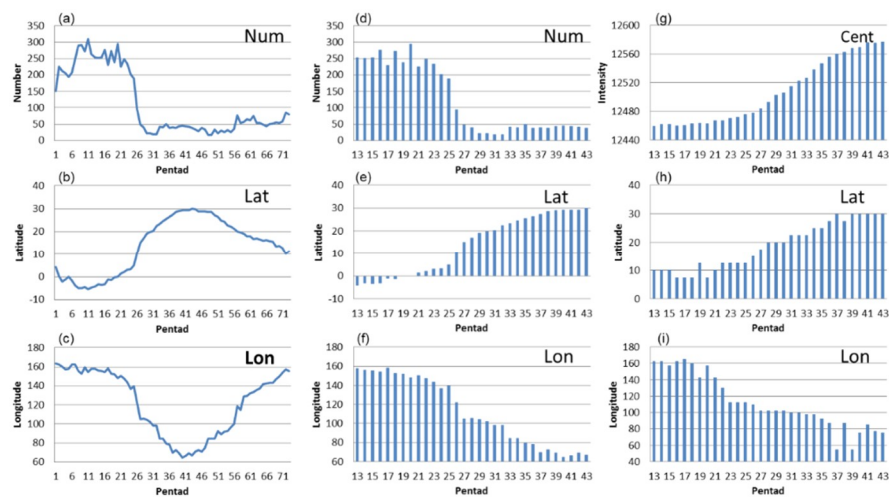


**Figure 3.** The pentad evolution of (a,d) the grid number in the region enclosed by the  $Z_{cent}$ -10 gpm contour, (b,e) the latitude and (c,f) longitude of SAH gravity center, (g) the maximum intensity, (h) the latitude and (i) longitude of maximum SAH center from (a–c) pentad 1–72 and (d–i) pentads 13–43.

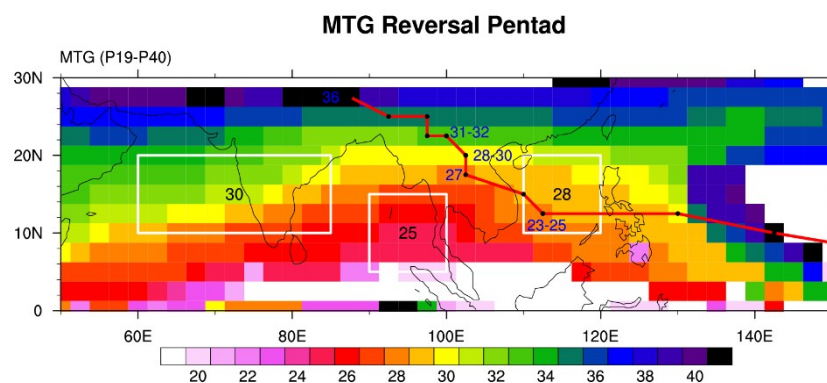


**Figure 4.** The transition pentads of the MTG from negative to positive during the spring-to-summer transition (P19–40) (shading; units: pentad) and the location of SAH maximum intensity center at 200 hPa (black dots) and the moving track (red lines) are also shown from Pentad 21 to Pentad 36. Pentads are shown by blue numbers. White boxes from West to East indicate the regions of ISM, BOB and SCS, respectively. Number inside each box is the domain average of the MTG transition pentads.

The mutual promotion of the SAH and ASM rainfall is important for the monsoon onset during the spring-to-summer transition. During early April from Pentad 19 to Pentad 22, the SAH is located over the Western Pacific. Convection over the Southern Philippines generates negative vorticity to the North in the upper level, which is transported to the SCS by the tropical upper Easterly [35,36]. Thus, the SAH center appears over the SCS on Pentad 23, two pentads before the ASM onset beginning in the BOB; then, it stays from Pentad 23 to Pentad 25 (Figures 2 and 4). Accompanying the strengthened SAH over the SCS, the Westerly wind is enhanced to its North. Both of the enhanced Westerly wind on the Northern flank and the weak Southerly wind on the Western flank of the SAH form the divergence in the Western SAH over the BOB (Figure 2e–g), in favor of the BOB monsoon onset on Pentad 25. After the BOB monsoon, the convection over the BOB triggers an anomalous anticyclone to its Northwest, which makes a sudden intensification (Figure 3d; grid number in  $Z_{cent}-10$  gpm contour suddenly decreases to below 100) and Northwestward shift (Figure 3h,i; from 12.5° N, 112.5° E to 15° N, 110° E) of the SAH. The gravity center of the SAH shifts from the Western Pacific (5.08° N, 139.5° E) to the Indochina Peninsula (15.15° N, 105.15° E) from Pentad 25 to Pentad 27 (Figure 3h–i), due to both the enhancement of geopotential height over the Indochina Peninsula and the weakening in its Eastern part over the Western North Pacific [35]. After the BOB monsoon onset, the latitude of gravity center almost coincides with that of maximum center (Figure 3e,h; less than 5° from Pentad 26 on), indicating the SAH maturing in its interaction with monsoon rainfall.

Due to the interaction of the SAH and monsoon rainfall in its South, the SAH is further strengthened and the Easterly wind in the positive MTG region (Southern flank of the SAH) is enhanced (Figure 2g–j). Both the enhanced Northeasterly wind on the Southern flank and the weak Northerly wind on the Eastern flank of the SAH form the divergence in the Eastern SAH over the SCS (Figure 2h–j), in favor of the SCS monsoon onset on Pentad 28 (Figure 4). After the SCS monsoon onsets, the SAH intensity is suddenly enhanced for the second time (Figure 3d; grid number in  $Z_{cent}-10$  gpm contour suddenly decreases to below 50). The latitude of maximum SAH center suddenly shifts to 20° N and stays there from Pentad 28 to Pentad 30 (Figure 3h). Being affected by the monsoon rainfall to its South in the positive MTG region, the SAH keeps growing with its gravity center moving Northwestward from Pentad 28 to Pentad 29 (Figure 3e–f). The maximum center greater than 12500 gpm appears over the Northern Indochina Peninsula (Figure 2k–i). On Pentad 29, the latitude of gravity center almost coincides with that of maximum center (Figure 3e,h; less than 1° from Pentad 29 on), indicating a matured SAH.

On Pentad 30, the SAH extends Westward significantly with the longitude of the West end of 12470 gpm shifting from 75° E to 60° E (Figure 2l). Accordingly, the ISM bursts in the West of the SAH. Most Asian region to the South of the SAH turns into summertime with the MTG higher than zero. The enhanced monsoon rainfall over Southern Asia keeps the SAH strengthening and moving Northwestward. After Pentad 36, the SAH moves onto the Tibetan Plateau and keeps its center near 27.5°–30° N (Figures 1 and 3). From then on, the SAH turns from moving stage to stable stage. The tropical ASM is fully established (Figure 4).

### 3.2. Key Factor Influencing the SAH Evolution

The Northward advancement of the SAH is closely related to the ASM onset. Climatologically, the ASM onsets in the BOB, the SCS and India appear from Pentad 25 to Pentad 30 in May. So, we define the SAH evolution index as the standardized latitude of the SAH gravity center in May, to investigate the inter-annual variation of the SAH and its relationship with the BOB monsoon, SCS monsoon and ISM onset. Based on the index, we chose six North track cases when the index is greater than one standard deviation and six South track cases when the index is less than  $-1$ . The evolution of the SAH gravity center from Pentad 19 to Pentad 36 in the North track cases and that in the South track cases are shown in Figure 5. When the index is greater than 1, the SAH gravity center propagates Northwestward from the Western Pacific (around 140°–150° E) to the Philippines on Pentad 22, and then keeps on shifting Northwestward from the Philippines to the East of central Indochina

Peninsula from its East coast on Pentad 28. We define this moving track as the North track of the SAH. When the index is less than  $-1$ , the SAH persists over the Western Pacific from Pentad 19 to Pentad 23. On Pentad 24, the SAH shifts Westward, instead of Northwestward, to Kalimantan Island and persists in the equatorial region to the South of  $10^{\circ}$  N until Pentad 27. On Pentad 28, the SAH shifts Northward to the Southern Indochina Peninsula from the Gulf of Thailand, and then keeps on moving Northwestward. This moving track is defined as the South track of the SAH. The North and South tracks show distinguished differences in term of time (Figures 5 and 6a), directions and locations (Figures 5 and 6) in the Northward advancement to the Indochina Peninsula for both gravity center and maximum center. These different Northward advancements of the SAH indicate different monsoon onset processes. Finding out the key factor influencing the SAH evolution can help better predict the tropical ASM onset.

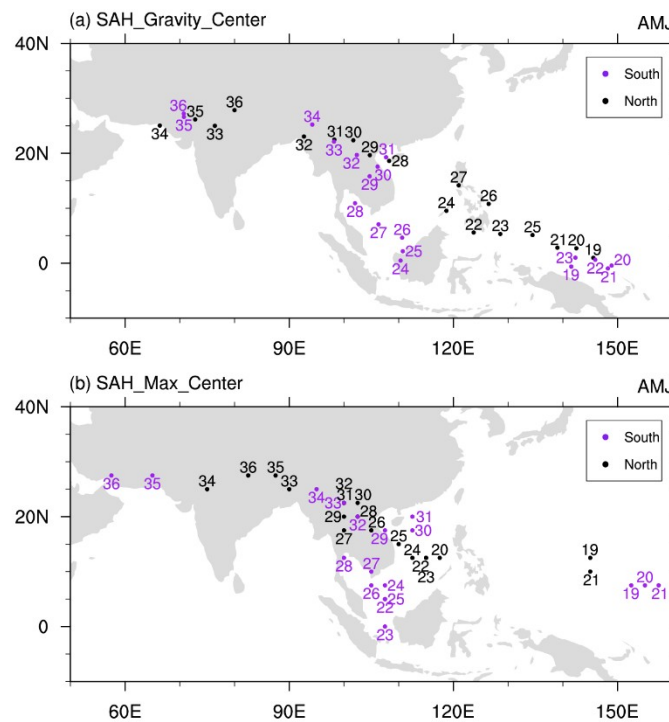


**Figure 5.** Locations of (a) SAH gravity centers and (b) SAH maximum center from Pentad 19 to Pentad 36 in the North (black dots) and South (purple dots) track cases. Black and purple numbers indicate the pentads in the North and South track cases, respectively.

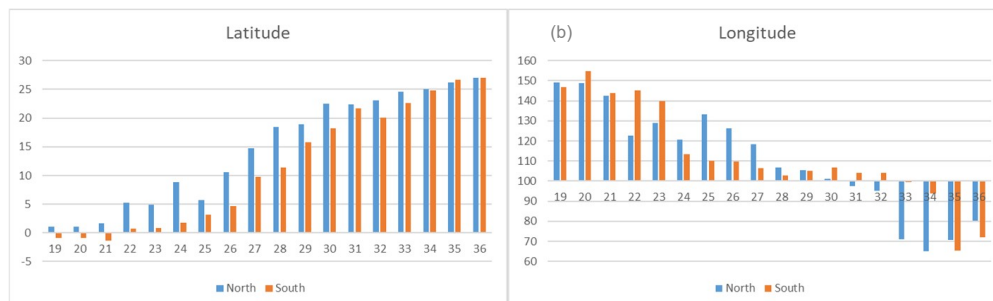


**Figure 6.** Composite evolutions of (a) latitude ( $^{\circ}$ N) and (b) longitude ( $^{\circ}$ E) of SAH gravity center from Pentad 19 to Pentad 36 for the North (blue) and South (orange) tracks.



Composite differences of SST and OLR in April associated with the SAH Northward advancement in May are shown in Figure 7. We can see the SAH development in the North/South track is closely related to the SST in the Western North Pacific and the tropical Indian Ocean, as well as the deep convection over the Philippines in previous month (Figure 7). In April, the warm SST in the Western Pacific favors stronger deep convection over the Philippines (Figure 7). The convection over the Southern Philippines produces a negative vorticity to its North, which is transported to the SCS by the tropical upper Easterly [36,39], leading to the Northwestward shift of the SAH from the Western Pacific to the SCS. However, in the South track cases, the colder SST in the Western Pacific suppresses the convection over the Southern Philippines, which is not conducive to the Northwestward shift of the SAH to the SCS. Meanwhile, the warmer SST in the tropical Indian Ocean induces an upper-level anticyclone in the tropics, which leads to the Westward shift of the SAH from the Western Pacific to Kalimantan Island and keeps the SAH persisting over the equatorial region with its center located to the South of  $10^{\circ}$  N for five pentads from Pentad 22 to Pentad 26 (Figure 5b). So, both the SST of the tropical Indian Ocean and Western North Pacific and the convection over the Southern Philippines are important for the Northwestward evolution of the SAH from the Western Pacific to the SCS.

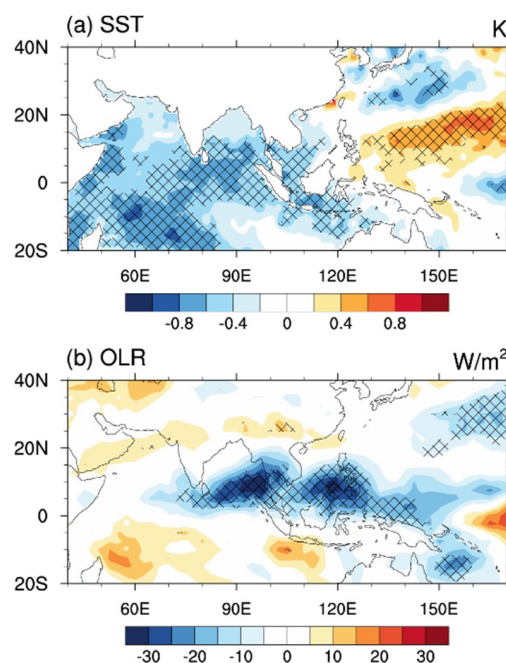


**Figure 7.** Composite differences of (a) SST anomalies (shading; K) and (b) OLR anomalies (shading;  $W/m^2$ ) in April between the North and South track cases. Cross hatching indicates the anomalies exceeding the 0.05 significance level.

### 3.3. Physical Process for the Mutual Promotion between the SAH and ASM Rainfall

Composite transition pentads of the MTG from negative to positive in the North and South track cases indicate different ASM onset processes associated with different evolutions of the SAH. In the North track cases, the summer circulation structure is established early over the BOB on Pentad 24, and then develops Northeastward and Northwestward gradually. The ASM onsets over both the SCS and ISM region are on Pentad 28, much earlier than normal (Figure 8a). In the South track cases, the ASM onset process is much later than normal. The summer circulation structure is established over the BOB, SCS and ISM region on pentads 27, 29, and 31, respectively (Figure 8b). The timing differences of onset pentads between the North and South track cases over BOB and ISM regions are 3 pentads, but 1 pentad over the SCS. Although only one pentad difference shown in the domain-average SCS monsoon onset time for the North and South track cases, but notable differences of onset process can be

found in the SCS region. In the North track cases, the monsoon onset advances Northward gradually over the SCS. However, in the South track cases, the monsoon bursts over the entire SCS on Pentad 29. So, we can find out significant differences in both the entire monsoon onset process and the individual monsoon onsets over these three typical monsoon regions. Similar result could be found by using ERA-interim data (figure not shown). This result indicates the ASM onset process is closely related to the Northward advancement of the SAH in the spring-to-summer transition: The entire ASM onset is much earlier in the North track cases than in the South track cases.

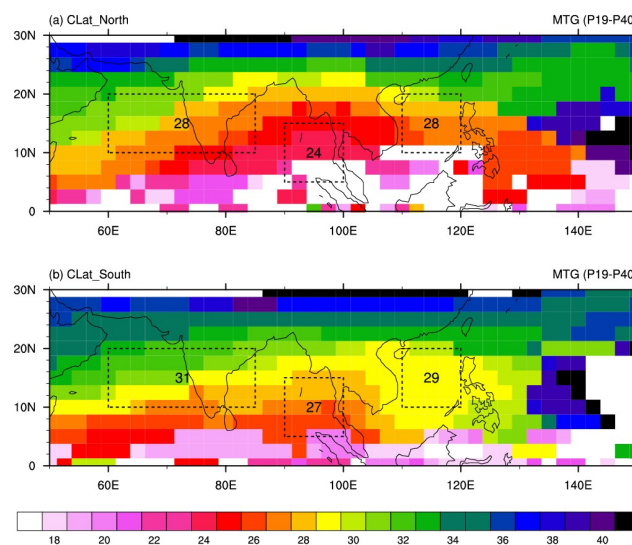


**Figure 8.** Composite transition pentads of the MTG from negative to positive in the (a) North and (b) South track cases (shading; units: pentad). Dashed boxes from West to East indicate the regions of the ISM, BOB and SCS, respectively. Number inside each box is the domain average of the MTG transition pentads.

The rainfall variation over the BOB, SCS and ISM region also suggests that the monsoon onset is much earlier in the North track cases than in the South track cases (Figure 9). On Pentad 24, the domain average of pentad rainfall over the BOB is suddenly enhanced from 4.37 mm/day to 9.32 mm/day in the North track cases. But in the South track cases, the sudden enhancement of rainfall occurs on Pentad 26 from 2.32 mm/day to 5.54 mm/day, and the rainfall amount reaches 7.54 mm/day on Pentad 27, both of which are later than those in the North track cases by about 2–3 pentads (Figure 9a). For the SCS, the abrupt rainfall increase occurs on Pentad 27 from 2.94 mm/day to 7.68 mm/day in the North track cases, which is earlier than that on Pentad 29 from 3.44 mm/day to 6.78 mm/day in the South track cases (Figure 9b). For the ISM rainfall, we can see an abrupt rainfall enhancement on Pentad 26 from 2.41 mm/day to 4.32 mm/day in the North track cases, which is earlier than that on Pentad 32 from 3.23 mm/day to 5.89 mm/day in the South track cases (Figure 9c). An all-India rainfall onset and demise (AIROD) index defined by Noska and Misra (2016) is further used to confirm the ISM onset pentad [10,56]. The result shows the monsoon onset over the ISM region on Pentad 28 and 31 for the North and South track cases, respectively, the same with that revealed by the MTG index. So, both the MTG and the rainfall indices reveal that the ASM evolutions are much earlier in the North track cases than in the South track cases of the SAH.

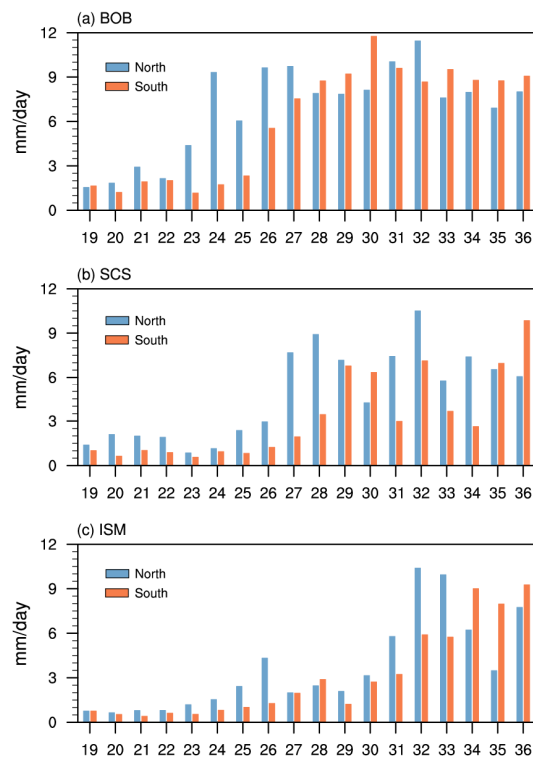


**Figure 9.** Composite rainfall over (a) the BOB ( $5^{\circ}$ – $15^{\circ}$  N,  $90^{\circ}$ – $100^{\circ}$  E), (b) SCS ( $10^{\circ}$ – $20^{\circ}$  N,  $110^{\circ}$ – $120^{\circ}$  E) and (c) ISM ( $10^{\circ}$ – $20^{\circ}$  N,  $70^{\circ}$ – $85^{\circ}$  E) from Pentad 19 to Pentad 36 in the Northward (blue bars) and Southward (orange bars) shift cases (mm/day).

The physical mechanism for the mutual promotion between the SAH evolution and monsoon rainfall is investigated by using the Easterly wind and the divergence in the upper level associated with the SAH, as well as the WNPSH in the mid level.

The Easterly wind on the South flank of the SAH is important for the establishment of the summer monsoon circulation and the formation of the upper-level divergence in the ASM regions. So, the Northward development of the SAH is crucial for the early or late onset of tropical summer monsoon. Figure 10 shows the establishment of the upper-level Easterly winds over the tropical ASM region along  $10^{\circ}$ – $20^{\circ}$  N. When the SAH develops in the North track, the reversal of zonal wind from Westerly to Easterly first appears over the BOB region ( $10^{\circ}$ – $20^{\circ}$  N,  $85^{\circ}$ – $105^{\circ}$  E) on Pentad 25, and then appears over the SCS ( $10^{\circ}$ – $20^{\circ}$  N,  $110^{\circ}$ – $120^{\circ}$  E) and ISM region ( $10^{\circ}$ – $20^{\circ}$  N,  $55^{\circ}$ – $85^{\circ}$  E) on Pentad 26 to Pentad 27 (Figure 10). The monsoonal circulation establishes over the BOB region ( $10^{\circ}$ – $20^{\circ}$  N,  $85^{\circ}$ – $105^{\circ}$  E) on around pentads 25–26, and over the SCS and the ISM region on Pentad 28 (Figure 8a), about one pentad later than the establishment of the Easterly wind. When the SAH propagates in the South track, the Northward shift of the SAH is much later. Thus, the Easterly wind establishes over the monsoon regions around Pentad 29, which is 2–3 pentads later than in the North track cases (Figure 10). As a result, the monsoon onsets over the ASM regions are late (i.e., Pentad 29 over the SCS and Pentad 31 over the ISM region; Figure 8b).

The evolution of upper-level divergence also shows the mutual promotion between the SAH and ASM rainfall. During early stage before the SAH shifting Northwestward to the SCS, the upper-level divergence first appears over the Indochina Peninsula ( $100^{\circ}$ – $110^{\circ}$  E) before Pentad 19 in the North track cases (Figure 11a). The upper-level divergence favors the convective activity over the Indochina Peninsula, and then facilitates the early advancement of the SAH from the Western Pacific to the SCS after Pentad 22 (Figure 5b). However, in the South track cases, the upper-level divergence is weak over the Indochina Peninsula during April from Pentad 19 to Pentad 24 (Figure 11b). It is unfavorable for the Northwestward shift of the SAH. Instead, the SAH shifts Westward to the South of the Indochina

Peninsula around Pentad 23, and then to the North of 10°N over the Southern Indochina Peninsula on Pentad 27 (Figure 5).

After the SAH advancing to the North of 10° N, the ASM bursts over the BOB. Figure 11 shows there are three stages of upper-level divergence occurring over the tropical Asia. In the North track cases, the upper-level divergence appears over the BOB (90°–100° E), SCS (110°–120° E), and ISM region (60°–85° E) on pentads 23, 26 and 28, respectively. In the South track cases, the upper-level divergence appears over these three regions on pentads 27, 28 and 30, respectively. The upper-level divergence leads 1–2 pentads before the monsoon onset. The upper-level divergence associated with the SAH at the entrance of the upper-level Easterly jet stream is important for the deep convection over the monsoon regions. Thus, we can see the sudden increases of monsoon rainfall in these regions appearing later correspondingly (Figure 9).

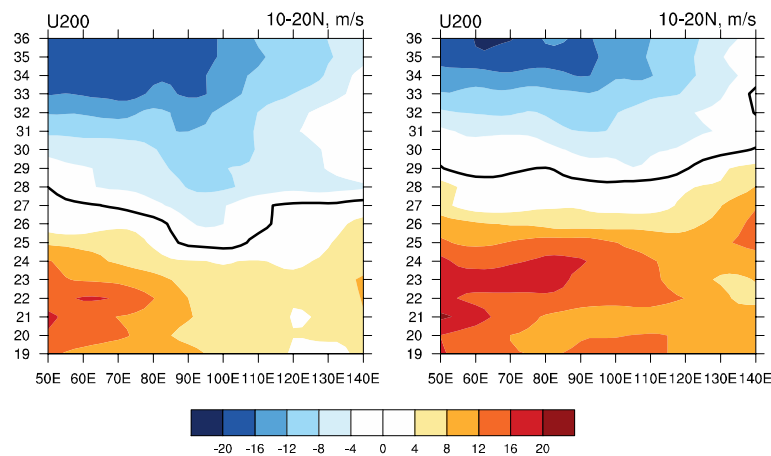


**Figure 10.** Hovmöller diagram of composite zonal wind at 200 hPa (shading; m/s) along 10°–20° N from Pentad 19 to Pentad 36 in the North (left) and South (right) track cases. Thick contour indicates zero.

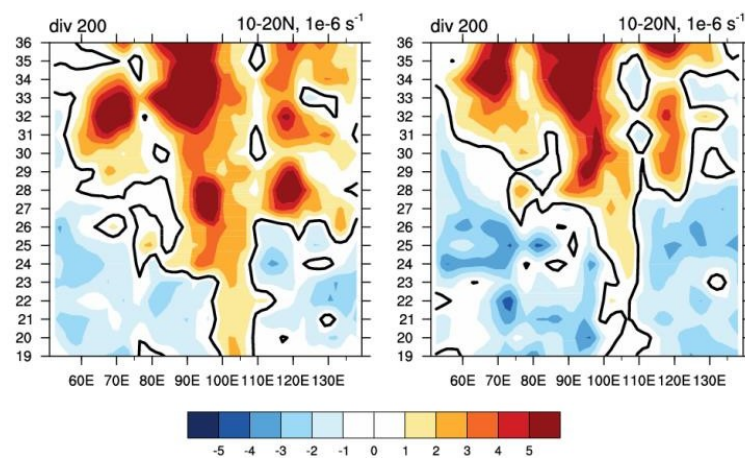


**Figure 11.** Hovmöller diagram of composite divergence at 200 hPa (shading;  $10^{-6} \text{ s}^{-1}$ ) along 10°–20° N from Pentad 19 to Pentad 36 in the North (left) and South (right) track cases. Thick contour indicates zero.

The Eastward retreat of the WNPSH is a key factor for the SCS monsoon onset. It can be identified as a sudden Eastward shift of the Western ridge of WNPSH from the SCS to the Western Pacific. Figure 12 shows the evolution of the 500-hPa geopotential height, and the Western ridge of WNPSH is highlighted by thick contours. The result shows sudden retreats of the Western ridge of subtropical high from the SCS (110°–120° E) to the Western Pacific (west of 130° E) occurs on Pentad 27 (Pentad 29) in the North (South) track cases, which is one pentad after the upper-level divergence appearing over

the SCS (Figure 11). On Pentad 26 (Pentad 28), the SAH gravity center shifts to the North of  $10^{\circ}$  N (Figure 6), and the maximum center is over the Indochina Peninsula in the North (South) track cases. So, the Easterly wind is enhanced to the South of the Indochina Peninsula. The SCS is located to the North of the entrance of the Easterly jet stream, where the upper-level divergence occurs (Figure 11). The upper-level divergence facilitates the ascending motion over the SCS, and a positive relative vorticity is formed in this region. As a result, the subtropical high retreats Eastward from the SCS to the Western Pacific on Pentad 27 (Pentad 29). Then, the Southwesterly wind carries abundant water vapor to the SCS, which leads to the SCS monsoon onset on Pentad 28 (Pentad 29) in the North (South) track cases.

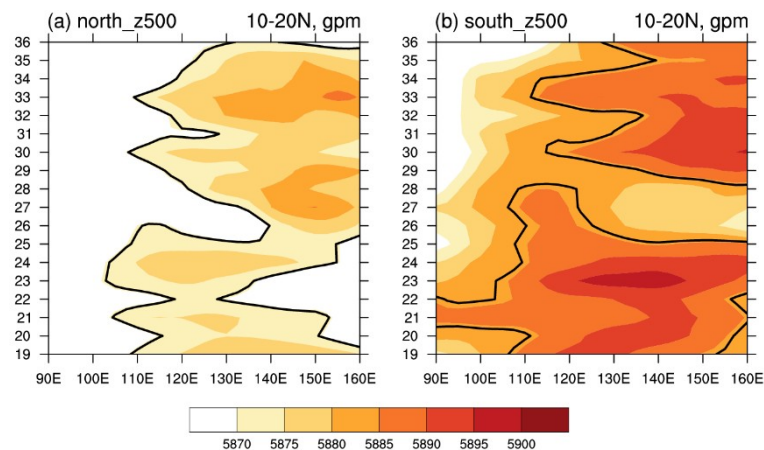


**Figure 12.** Hovmöller diagram of composite geopotential height at 500 hPa (shading: gpm) along  $10^{\circ}$ – $20^{\circ}$  N from Pentad 19 to Pentad 36 in the North (**left**) and South (**right**) track cases. The average geopotential height in the North (**a**, 5870.49 gpm) and South (**b**, 5883.98 gpm) track cases over the SCS ( $10^{\circ}$ – $20^{\circ}$  N,  $110^{\circ}$ – $120^{\circ}$  E) during Pentad 19 to Pentad 36 are highlighted by thick contours, which indicate the Western ridge of the WNPSH.

#### 4. Conclusions

The evolution of the SAH and its role in the ASM onset process during spring-to-summer transition are investigated by using the NCEP-DOE reanalysis data II. Results show that the Northwestward evolution of the SAH from the Western Pacific to the SCS, the Indochina Peninsula and the South Asian plateaus, is closely related with the ASM onsets over the BOB, SCS, and ISM region. Climatologically, there are four sudden changes of the SAH on pentads 23, 27, 29 and 31, respectively. On Pentad 23, the SAH shifts Westward suddenly to the SCS, due to the convection over the Southern Philippines. The associated divergence on the Western flank of the SAH enhances ascending motion to the West of the SAH and results in the ASM onset over the BOB on Pentad 25. Condensational latent heat associated with the BOB monsoon rainfall excites an anticyclone to its Northwest, which favors the Northwestward development of the SAH. On Pentad 27, the SAH intensity is strengthened rapidly and the center shifts to the Indochina Peninsula. The Easterly wind associated with the enhanced SAH on its Southern flank is intensified accordingly. So, the upper-level divergence is formed over the SCS at the entrance of the Easterly jet stream. The upper-level divergence favors the ascending motion over the SCS, and also leads to the Eastward retreatment of the WNPSH, which results in the monsoon onset over the SCS. After the SCS monsoon onset on Pentad 28, the convective activity over the SCS further strengthens the SAH to over 12500 gpm and the SAH center shifts Northward to  $20^{\circ}$  N over the Northern Indochina Peninsula on Pentad 29. Accompanying the strengthened and Northward shifted SAH, the Easterly wind on its Southern flank is strengthened and shifts Northward. On Pentad 30, the Easterly wind is established over the ISM region. The upper-level Easterly wind and lower-level Southwesterly wind form the summer-type baroclinic vertical structure over the ISM region and the ISM onset occurs. On Pentad 31, the convection in the ISM region further strengthens the SAH to

its Northwest. Both the maximum center and the gravity center of the SAH shift to the Northwest of 20° N, 100° E. The mutual promotion of the SAH and ASM rainfall supports the Northwestward development of the SAH to the South Asian plateaus until Pentad 37. After that, the SAH turns from moving stage to stable stage with robust and slightly varied intensity and the SAH center hovers around 27.5°–30° N over the plateaus.

External forcing affecting the SAH evolution in the spring-to-summer transition is also investigated, with a focus on the interannual time scale. The SSTs in the Western Pacific and tropical Indian Ocean in the previous month (i.e., April) play important roles in the Northward advancement of the SAH. Warmer SST in the Western Pacific leads to more intense deep convection over the Southern Philippines, which favors the Northwestward shift of the SAH to the SCS and triggers the mutual promotion between the SAH and ASM earlier. However, when the convection over the Philippines is inactive, the Northwestward shift of the SAH will be delayed. The warmer SST in the tropical Indian Ocean can excite an anomalous anticyclone near the equator according to the Gill-type response, which leads to a Westward shift of the SAH instead of a Northwestward shift, and keeps the SAH in the lower latitudes. The delayed Northward shift of the SAH will postpone the establishment of the Easterly winds and the divergence at the upper level over the ASM regions. As a result, the monsoon circulation builds up later than normal, and the monsoon rainfall increases later correspondently.

**Author Contributions:** Conceptualization, W.W., S.Y. and W.Z.; methodology, W.W. and Y.W.; software, W.W. and Y.W.; investigation, W.W. and Y.W.; writing—original draft preparation, W.W.; writing—review and editing, W.W., S.Y., and W.Z.; visualization, Y.W. and W.W.

**Funding:** This research was funded by the National Natural Science Foundation of China (Grant 41605040, 41661144019 and 91637208), the “111-Plan” Project of China (B17049) and the Key Laboratory of Meteorological Disaster of Ministry of Education (KLME1504).

**Acknowledgments:** NCEP\_Reanalysis II data and Interpolated OLR data used in this study are provided by the NOAA/OAR/ESRL PSD, Boulder, Colorado, USA (<https://www.esrl.noaa.gov/psd/>). Global Precipitation Climatology Project (GPCP) Version 2.2 pentad data are provided by the NASA (<https://precip.gsfc.nasa.gov/>).

**Conflicts of Interest:** The authors declare no conflict of interest.

## References

1. Mason, R.B.; Anderson, C.E. The Development and Decay of the 100mb Summertime Anticyclone over Southern Asia. *Mon. Weather Rev.* **1963**, *91*, 3–12. [[CrossRef](#)]
2. Tao, S.; Zhu, F. The 100-mb flow patterns in Southern Asia in summer and its relation to the advance and retreat of the West-Pacific subtropical anticyclone over the Far East. *Acta Meteorol. Sin.* **1964**, *34*, 385–396.
3. Krishnamurti, T.N.; Bhalme, H. Oscillations of a monsoon system. Part I. Observational aspects. *J. Atmos. Sci.* **1976**, *33*, 1937–1954. [[CrossRef](#)]
4. Tao, S.; Chen, L. A Review of Recent Research on the East Asian Summer Monsoon in China. In *Monsoon Meteorology*; Chang, C.-P., Krishnamurti, T.N., Eds.; Oxford University Press: Oxford, UK, 1987; pp. 60–92.
5. Wei, W.; Zhang, R.; Wen, M. Meridional variation of South Asian High and its relationship with the summer precipitation over China. *J. Appl. Meteorol. Sci.* **2012**, *23*, 650–659.
6. Wei, W.; Zhang, R.; Wen, M.; Rong, X.; Li, T. Impact of Indian summer monsoon on the South Asian High and its influence on summer rainfall over China. *Clim. Dyn.* **2014**, *43*, 1257–1269. [[CrossRef](#)]
7. Wei, W.; Zhang, R.; Wen, M.; Kim, B.-J.; Nam, J.-C. Interannual Variation of the South Asian High and Its Relation with Indian and East Asian Summer Monsoon Rainfall. *J. Clim.* **2015**, *28*, 2623–2634. [[CrossRef](#)]
8. Wei, W.; Zhang, R.; Wen, M.; Yang, S. Relationship between the Asian Westerly Jet Stream and Summer Rainfall over Central Asia and North China: Roles of the Indian Monsoon and the South Asian High. *J. Clim.* **2017**, *30*, 537–552. [[CrossRef](#)]
9. Xue, X.; Chen, W.; Chen, S.; Zhou, D. Modulation of the connection between boreal winter ENSO and the South Asian high in the following summer by the stratospheric quasi-biennial oscillation. *J. Geophys. Res. Atmos.* **2015**, *120*, 7393–7411. [[CrossRef](#)]
10. Noska, R.; Misra, V. Characterizing the onset and demise of the Indian summer monsoon. *Geophys. Res. Lett.* **2016**, *43*, 4547–4554. [[CrossRef](#)]

11. Shi, J.; Qian, W. Connection between Anomalous Zonal Activities of the South Asian High and Eurasian Summer Climate Anomalies. *J. Clim.* **2016**, *29*, 8249–8267. [[CrossRef](#)]
12. Zhang, P.; Liu, Y.; Lu, J. Impact of East Asian Summer Monsoon on the Interannual Variation of South Asian High. *J. Clim.* **2016**, *29*, 159–173. [[CrossRef](#)]
13. Liu, Y.; Wang, Z.; Zhuo, H.; Wu, G. Two types of summertime heating over Asian large-scale orography and excitation of potential-vorticity forcing II. Sensible heating over Tibetan-Iranian Plateau. *Sci. China Earth Sci.* **2017**, *60*, 733–744. [[CrossRef](#)]
14. Wang, L.; Dai, A.; Guo, S.; Ge, J. Establishment of the South Asian high over the Indo-China Peninsula during late spring to summer. *Adv. Atmos. Sci.* **2017**, *34*, 169–180. [[CrossRef](#)]
15. Xue, X.; Chen, W.; Chen, S.F. The climatology and interannual variability of the South Asia high and its relationship with ENSO in CMIP5 models. *Clim. Dyn.* **2017**, *48*, 3507–3528. [[CrossRef](#)]
16. Xue, X.; Chen, W.; Chen, S.; Feng, J. PDO modulation of the ENSO impact on the summer South Asian high. *Clim. Dyn.* **2018**, *50*, 1393–1411. [[CrossRef](#)]
17. Li, H.; He, S.; Fan, K.; Wang, H. Relationship between the onset date of the Meiyu and the South Asian anticyclone in April and the related mechanisms. *Clim. Dyn.* **2019**, *52*, 209–226. [[CrossRef](#)]
18. Krishnamurti, T. Summer monsoon experiment—A review. *Mon. Weather Rev.* **1985**, *113*, 1590–1626. [[CrossRef](#)]
19. Krishnamurti, T. Tropical east-west circulations during the northern summer. *J. Atmos. Sci.* **1971**, *28*, 1342–1347. [[CrossRef](#)]
20. Krishnamurti, T. Observational study of the tropical upper tropospheric motion field during the Northern Hemisphere summer. *J. Appl. Meteorol.* **1971**, *10*, 1066–1096. [[CrossRef](#)]
21. Bansod, S.D.; Yin, Z.Y.; Lin, Z.; Zhang, X. Thermal field over Tibetan Plateau and Indian summer monsoon rainfall. *Int. J. Climatol.* **2003**, *23*, 1589–1605. [[CrossRef](#)]
22. Ashfaq, M.; Shi, Y.; Tung, W.; Trapp, R.J.; Gao, X.; Pal, J.S.; Diffenbaugh, N.S. Suppression of south Asian summer monsoon precipitation in the 21st century. *Geophys. Res. Lett.* **2009**, *36*. [[CrossRef](#)]
23. Yanai, M.; Wu, G.X. Effects of the Tibetan Plateau. In *The Asian Monsoon*; Springer Praxis Books; Springer: Berlin/Heidelberg, Germany, 2006; pp. 513–549.
24. Koteswaram, P. The Easterly Jet Stream in the Tropics. *Tellus* **1958**, *10*, 43–57. [[CrossRef](#)]
25. Ren, X.; Yang, D.; Yang, X.-Q. Characteristics and Mechanisms of the Subseasonal Eastward Extension of the South Asian High. *J. Clim.* **2015**, *28*, 6799–6822. [[CrossRef](#)]
26. Chen, Y.; Zhai, P. Mechanisms for concurrent low-latitude circulation anomalies responsible for persistent extreme precipitation in the Yangtze River Valley. *Clim. Dyn.* **2016**, *47*, 989–1006. [[CrossRef](#)]
27. Guan, W.; Ren, X.; Shang, W.; Hu, H. Subseasonal Zonal Oscillation of the Western Pacific Subtropical High during Early Summer. *J. Meteorol. Res.* **2018**, *32*, 768–780. [[CrossRef](#)]
28. Krishnamurti, T.N.; Daggupati, S.M.; Fein, J.; Kanamitsu, M.; Lee, J.D. Tibetan high and upper tropospheric tropical circulation during northern summer. *Bull. Am. Meteorol. Soc.* **1973**, *54*, 1234–1249. [[CrossRef](#)]
29. Yang, H.; Sun, S. Longitudinal displacement of the subtropical high in the western Pacific in summer and its influence. *Adv. Atmos. Sci.* **2003**, *20*, 921–933.
30. Ren, R.; Wu, G. On the short-term structure and formation of the subtropical anticyclone in the summer of 1998. *Acta Meteorol. Sin.* **2003**, *61*, 180–195.
31. Wu, G.; Duan, A.; Liu, Y.; Mao, J.; Ren, R.; Bao, Q.; He, B.; Liu, B.; Hu, W. Tibetan Plateau climate dynamics: Recent research progress and outlook. *Natl. Sci. Rev.* **2015**, *2*, 100–116. [[CrossRef](#)]
32. Wu, R.; Wang, B. Multi-stage onset of the summer monsoon over the western North Pacific. *Clim. Dyn.* **2001**, *17*, 277–289. [[CrossRef](#)]
33. Wang, B. The Time-Space Structure of the Asian-Pacific Summer Monsoon: A Fast Annual Cycle View. *J. Clim.* **2002**, *15*, 2001–2019. [[CrossRef](#)]
34. Wu, R. Subseasonal variability during the South China Sea summer monsoon onset. *Clim. Dyn.* **2009**, *34*, 629–642. [[CrossRef](#)]
35. Liu, B.; He, J.; Wang, L. Characteristics of the South Asia high establishment processes above the Indo-China Peninsula from April to May and their possible mechanism. *Chin. J. Atmos. Sci.* **2009**, *33*, 1319–1332.
36. Liu, B.; Wu, G.; Mao, J.; He, J. Genesis of the South Asian High and Its Impact on the Asian Summer Monsoon Onset. *J. Clim.* **2013**, *26*, 2976–2991. [[CrossRef](#)]

37. Wu, G.; Ren, S.; Xu, J.; Wang, D.; Bao, Q.; Liu, B.; Liu, Y. Impact of tropical cyclone development on the instability of South Asian High and the summer monsoon onset over Bay of Bengal. *Clim. Dyn.* **2013**, *41*, 2603–2616. [[CrossRef](#)]
38. Liu, B.; He, J.; Wang, L. On a possible mechanism for southern Asian convection influencing the South Asian high establishment during winter to summer transition. *J. Trop. Meteorol.* **2012**, *18*, 473–484.
39. He, J.; Liu, B.; Wu, G. Formation of South Asia high from late spring to early summer and its association with ENSO events. *Chin. J. Atmos. Sci.* **2014**, *38*, 670–684. [[CrossRef](#)]
40. Liu, B.; Wu, G.; Ren, R. Influences of ENSO on the vertical coupling of atmospheric circulation during the onset of South Asian summer monsoon. *Clim. Dyn.* **2015**, *45*, 1859–1875. [[CrossRef](#)]
41. Wang, B.; Zhang, Y.S.; Lu, M.M. Definition of South China Sea monsoon onset and commencement of the East Asia summer monsoon. *J. Clim.* **2004**, *17*, 699–710. [[CrossRef](#)]
42. Zhou, W.; Chan, J.C. ENSO and the South China Sea summer monsoon onset. *Int. J. Climatol.* **2007**, *27*, 157–167. [[CrossRef](#)]
43. Zhou, W.; Chan, J.C.L. Intraseasonal oscillations and the South China Sea summer monsoon onset. *Int. J. Climatol.* **2005**, *25*, 1585–1609. [[CrossRef](#)]
44. Webster, P.J.; Yang, S. Monsoon and ENSO: Selectively interactive systems. *Q. J. R. Meteorol. Soc.* **1992**, *118*, 877–926. [[CrossRef](#)]
45. Wang, B.; Wu, Z.; Li, J.; Liu, J.; Chang, C.-P.; Ding, Y.; Wu, G. How to Measure the Strength of the East Asian Summer Monsoon. *J. Clim.* **2008**, *21*, 4449–4463. [[CrossRef](#)]
46. Yang, H.; Li, C.Y. Effect of the tropical Pacific-Indian Ocean temperature anomaly mode on the South Asia High. *Chin. J. Atmos. Sci.* **2005**, *29*, 99–110.
47. Yang, J.; Liu, Q. The “charge/discharge” roles of the basin-wide mode of the Indian Ocean SST anomaly—Influence on the South Asia High in summer. *Acta Oceanol. Sin.* **2008**, *30*, 12–19.
48. Zhou, T.J.; Yu, R.C.; Zhang, J.; Drange, H.; Cassou, C.; Deser, C.; Hodson, D.L.R.; Sanchez-Gomez, E.; Li, J.; Keenlyside, N.; et al. Why the Western Pacific Subtropical High Has Extended Westward since the Late 1970s. *J. Clim.* **2009**, *22*, 2199–2215. [[CrossRef](#)]
49. Huang, G.; Qu, X.; Hu, K.M. The Impact of the Tropical Indian Ocean on South Asian High in Boreal Summer. *Adv. Atmos. Sci.* **2011**, *28*, 421–432. [[CrossRef](#)]
50. Kanamitsu, M.; Ebisuzaki, W.; Woollen, J.; Yang, S.K.; Hnilo, J.J.; Fiorino, M.; Potter, G.L. NCEP–DOE AMIP-II Reanalysis (R-2). *Bull. Am. Meteorol. Soc.* **2002**, *83*, 1631–1643. [[CrossRef](#)]
51. Liebmann, B.; Smith, C.A. Description of a complete (interpolated) outgoing longwave radiation dataset. *Bull. Am. Meteorol. Soc.* **1996**, *77*, 1275–1277.
52. Mao, J.Y.; Chan, J.C.L.; Wu, G.X. Relationship between the onset of the South China Sea summer monsoon and the structure of the Asian subtropical anticyclone. *J. Meteorol. Soc. Jpn.* **2004**, *82*, 845–859. [[CrossRef](#)]
53. Li, C.; Yanai, M. The Onset and Interannual Variability of the Asian Summer Monsoon in Relation to Land-Sea Thermal Contrast. *J. Clim.* **1996**, *9*, 358–375. [[CrossRef](#)]
54. Webster, P.J.; Magaña, V.O.; Palmer, T.N.; Shukla, J.; Tomas, R.A.; Yanai, M.; Yasunari, T. Monsoons: Processes, predictability, and the prospects for prediction. *J. Geophys. Res.* **1998**, *103*, 14451–14510. [[CrossRef](#)]
55. Mao, J.; Wu, G. Interannual variability in the onset of the summer monsoon over the Eastern Bay of Bengal. *Theor. Appl. Climatol.* **2007**, *89*, 155–170. [[CrossRef](#)]
56. Misra, V.; Bhardwaj, A.; Mishra, A. Local onset and demise of the Indian summer monsoon. *Clim. Dyn.* **2018**, *51*, 1609–1622. [[CrossRef](#)]

